In This Issue

A Key to Regulation of One Carbon Metabolism

PAGE 1375

Ren et al. report on the structure of the ZMP-bound *T. carboxydivorans pfl* riboswitch, thereby defining the pseudoknot-based tertiary RNA fold, the binding pocket architecture and principles underlying ligand recognition specificity. The study highlights the RNA-based recognition of ZMP, a master regulator of one-carbon metabolism.

Allosteric Conformational Changes in BRAF/RAS Relationship

PAGE 1382

RAS binding is a critical step in the activation of BRAF kinase and the MAPK signaling pathway. Aramini et al. report the solution NMR and X-ray crystal structures of the RAS-binding domain (RBD) from human BRAF and use NMR to reveal unexpected allosteric changes in BRAF RBD upon RAS binding.

How Mitochondrial SCaMC Carrier Selects MgATP

PAGE 1394

The AAC and SCaMC are two major nucleotide carriers responsible for transporting ATP/ADP and metal-complexed ATP/ADP across the mitochondrial inner membrane. Run et al. revealed a structural differences between the two homologs, which explains SCaMC's higher selectivity for transporting MgATP over ATP compared to AAC.

TRPV Channels: Keeping Things Intramolecular

PAGE 1404

Transient receptor potential (TRP) cationic channels are important cellular sensors of the environment. Garcia-Elias et al. show that the interactions among different domains of the same subunit are structural determinants of TRP channel folding and assembly.

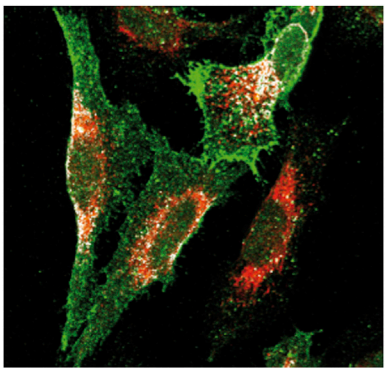

Atomic Model of an Immature Gag Lattice

PAGE 1414

Goh et al. present an atomic model of the Gag lattice, using RSV as the model virus. Construction of the model is based on cryo-EM densities of M-PMV, together with high-resolution structures of RSV. Validity of the model is evaluated by MD simulations, biochemical experiments, and structural comparison with the immature capsid of HIV.

Structural View of CD6 and Its Ligand CD166

PAGE 1426

Chappell et al. present structures of the T cell surface receptor CD6, the first of consecutive scavenger receptor cysteine rich domains, and its ligand CD166. The data provide mechanisms for competition between CD166 homophilic and heterophilic interactions and perturbation of function by SNPs and mAbs.

How Roquin Finds Its RNA

PAGE 1437

The protein Roquin recognizes CDE-type stem-loops of mRNA in a sequence specific manner. Codutti et al. describe distinct features of the solution structures of the unbound TNF-α CDE and of a non-functional mutant, which recapitulate their different Roquin-binding abilities and allow proposing a revised consensus motif for prediction of new CDE stem-loops.

Tracking Down Effects of Tau Phosphorylation

PAGE 1448

Alzheimer disease-related protein Tau is a phosphoprotein, and a number of different residues are subject to phosphorylation. Schwalbe et al. develop a molecular ensemble approach and use it to reveal an atomic-level description of the phosphorylation-induced structural changes in Tau phosphorylated at Thr231.

In This Issue

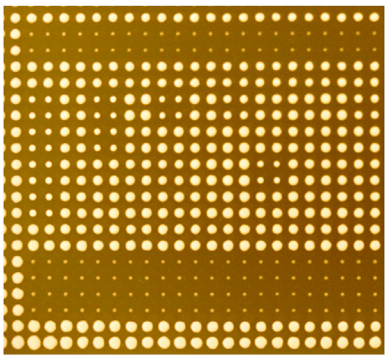

How Pathogens Hijack Host's Ubiquitination Cascade

PAGE 1459

Legionella effector LubX functions as a ubiquitin protein ligase inside the host cell. Quaile et al. provide the first molecular structure of this protein and its complex with human UBE2D2. This data is used to gain insight into molecular function of this pathogenic factor.

Bacterial RNA Polymerase: New Inhibitors, New Hope

PAGE 1470

CBR hydroxamidines and CBR pyrazoles inhibit Gram-negative bacterial RNA polymerase (RNAP) and exhibit antibacterial activity against Gram-negative bacteria. Feng et al. report crystal structures of CBRs bound to *Escherichia coli* RNAP and define structural, mechanistic, cross-resistance, and additivity relationships between CBRs and other RNAP inhibitors.

Structure of Human Neutral Ceramidase

PAGE 1482

Neutral ceramidase regulates the balance of ceramide and S1P: two bioactive lipids with opposing effects on cancer cell growth. Airola et al. define the structure of this enzyme, the first for a eukaryotic ceramide-metabolizing enzyme, and reveal how this therapeutic target hydrolyzes and recognizes ceramide.

Control of Actin Assembly in Budding Yeast

PAGE 1492

In budding yeast, Bud6 partners with formins Bni1 and Bnr1 to catalyze assembly of actin filaments. The crystal structure of a fragment of Bud6 in complex with actin, described by Park et al., reveals striking similarities with the WH2 motif, an actin-binding element found in WASP and other proteins that control actin assembly.

Glimpsing at Regulation of Lipopolysaccharide Synthesis

PAGE 1500

The molecular mechanism behind the regulation of lipopolysaccharide syntheses regulation by LapB is currently unclear. Prince and Jia present structure of LapB. LapB contains nine TPR motifs and a rubredoxin-type metal binding domain. The relationship between these structural motifs appears essential for function.

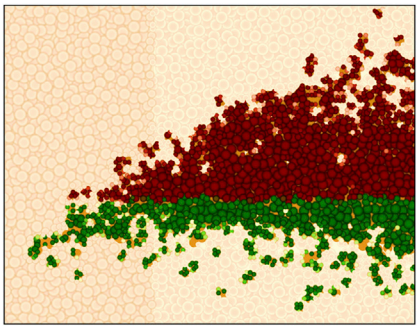

Fatal pepATTRACT-Ion

PAGE 1507

Schindler et al. present the fully blind peptide-protein docking protocol pepATTRACT. pepATTRACT predicts both the binding site and the bound peptide conformation to high precision simultaneously. It has the potential for proteome-wide applications.

For Limited Structural Datasets try SPECTRUS

PAGE 1516

Ponzoni et al. present SPECTRUS, a general method to identify dynamical domains in proteins. SPECTRUS uses a dimensional reduction of the inter-residue distance fluctuations and exploits its properties to single out the intrinsic number and type of domains.

For Electrostatics of Membrane Proteins Try APBSmem

PAGE 1526

Marcoline et al. highlight major new features to a software program, APBSmem, which allows users to carry out electrostatics calculations on membrane proteins and membrane-associated proteins. The authors use APBSmem to reveal new biological information concerning several proteins of interest.

In This Issue

Hands Up, Human Genome, GPCR-I-TASSER Is Pointed at You

PAGE 1538

Zhang et al. develop a hybrid approach, GPCR-I-TASSER, for GPCR structure predictions, which combines experimental mutagenesis data with ab initio transmembrane helix assembly simulations. The method was applied to 1026 GPCRs in the human genome, with successfully modeled targets containing many pharmaceutically important families with no previously solved structures.

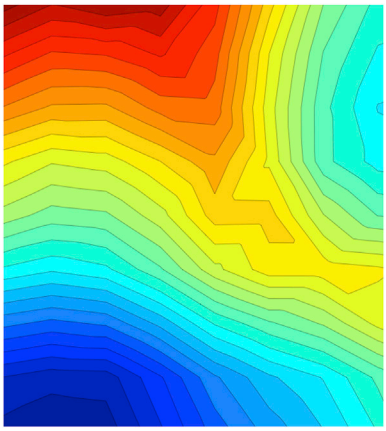

Recruiting NH_4^+, but Transporting NH_3

PAGE 1550

Using molecular and quantum mechanic simulations, Baday et al. show that the RhCG protein transports NH_3 but actually recruits NH_4^+. The substrate transfers a proton to a signature histidine and diffuses further as NH_3. The transferred proton is shuttled back to the extracellular side, resulting in a net electroneutral transport.

